

# TECHNOLOGY PROGRESS AND IN-ORBIT DEMONSTRATION OF ELECTRODYNAMIC TETHERS IN THE FRAMEWORK OF THE E.T.PACK INITIATIVE

G. Sánchez-Arriaga<sup>(1)</sup>, M. Tajmar<sup>(2)</sup>, A. Valmorbida<sup>(3)</sup>, X. Ezara<sup>(4)</sup>, E. Kiema<sup>(5)</sup>, and J. Muñoz Tejada<sup>(6)</sup>

<sup>(1)</sup>Universidad Carlos III de Madrid, Avenida de la Universidad 30, 28911, Leganés, Spain, Email: gonzalo.sanchez@uc3m.es

<sup>(2)</sup>Technische Universität Dresden, Marschnerstr. 32, 01307 Dresden, Germany, Email: martin.tajmar@tu-dresden.de

<sup>(3)</sup>CISAS “G.Colombo” and Department of Industrial Engineering (DII), University of Padua, Padua, Italy, Email: andrea.valmorbida@unipd.it

<sup>(4)</sup>Sener Aeroespacial S.A, Calle Severo Ochoa 4, Tres Cantos, 28760, Spain, Email: xunqueira.ezara@aeroespacial.sener

<sup>(5)</sup>Rocket Factory Augsburg, Berliner Allee 65, 86153 Augsburg, Germany, Email: elsie.kiema@rfa.space

<sup>(6)</sup>PERSEI Space, Avenida Gregorio Peces-Barba 1, 28918 Leganés, Spain, Email: jesus.munoz.tejada@perseispace.com

## ABSTRACT

The results of the qualification campaign of the engineering qualification model of a 12 U and 20 kg deorbit device based on electrodynamic tether (EDT) technology are presented. The campaign included pressure, leak, functional, partial tether deployment, vibration, shock, thermal vacuum cycling, electromagnetic compatibility, module separation, and full tether deployment tests. The flight model of the deorbit device is currently under development and will pass the acceptance test campaign in Q3 2025. The flight of the DD, planned in an orbit of 49° of inclination and about 550 km of altitude, is scheduled in Q2 2026.

Keywords: Electrodynamic Tethers, Deorbit Technologies..

## 1. INTRODUCTION

Active Debris Removal (ADR) and Post-Mission Disposal (PMD) are two examples of orbital debris remediation actions that can benefit extraordinarily from a robust and autonomous Deorbit Device (DD). For instance, an in-orbit servicing vehicle can capture and install DDs on debris for their later autonomous deorbiting. By using DDs based on solid propellant, a platform with a wet mass of 2000 kg and a dry mass of 600 kg could deorbit 35 rocket bodies from sun-synchronous orbit within the nominal 7 years spacecraft life time with 8 resupply operations [4]. Regarding PMD, equipping future satellites with no propulsion capabilities in Low Earth Orbit with an autonomous DD for its deorbiting at the end of life seems to be an effective solution to meet the 5-year post mission disposal time already adopted by the Federal Communication Commission [6] and considered in

ESA's Zero Debris approach. Even if the satellite has a propulsion system, adding an autonomous deorbit device can be an interesting option to have a backup system.

There is a need for having access to autonomous and light DDs, but preparing them is challenging from a technological point of view. For instance, an autonomous and light DD based on electric propulsion seems to be very difficult due to the required power and the complexity. Regarding solid propellant, the D-Sat mission by D-Orbit was the first satellite ever designed to be removed from orbit by means of a dedicated and independent propulsive decommissioning device. All subsystems of the decommissioning device were verified in space. However, due to mounting misalignments and possibly combustion instabilities which may deviate the thrust vector during the fire, the disposal maneuver was not nominal and the D-SAT post fire orbit was about 100 km higher than the original one [7].

Due to their passive character, drag sails are an alternative to prepare autonomous DDs and important technological progress was achieved in the last years [1]. For objects at orbits whose natural decay time is slightly above the 5-year, sails can make them compliant. However, the area-time product, which is an important figure of merit related to the collision risk, is kept invariant by sails. It is also unlikely that sails will be used for deorbiting large satellites from altitudes around 800 km because the very low air density makes them ineffective. Electrodynamic Tethers (EDTs), like sails, are passive and propellant-less, reduce the time-to-area product and are effective in a broad range of orbit altitudes and inclinations [12]. Both the passive aerodynamic and electrodynamic (Lorentz) drags act on EDTs, being typically the latter much larger than the former.

Although about 27 missions with conductive tethers were carried out in suborbital and orbital flights, a bare tether [16] equipped with a hollow cathode has been never

demonstrated in an orbital flight [14]. Such a tether configuration is the one that offers the best performance and, therefore, it is the most promising for preparing autonomous DDs targeted to deorbit medium and large space debris (above hundreds of kg). The Plasma Motor Generator mission, flown by NASA in 1993, used an insulated tether with two hollow cathodes and successfully demonstrated the two operation modes of an EDT (Generator and Motor Modes) [9]. In Europe, the two recent EIC-funded E.T.PACK and E.T.PACK-F projects allowed to increase the Technology Readiness Level (TRL) of EDTs. The former prepared a prototype with TRL 4 [13] and the latter is preparing a flight ready DD [15]. Its in-orbit demonstration is scheduled in Q2 2026, thanks to a launch provided by AVIO and supported by the ESA/EC flight Tickets Initiative.

This work presents the results of the qualification campaign of the Engineering Qualification Model (EQM) of the DD of the E.T.PACK-F project. Section 2 presents the main features of the DD and Section 3 the test plan. Section 4 shows the results of the tests. The conclusions are summarized in Section 5.

## 2. THE DEORBIT DEVICE

The EQM has a mass of 20 kg and a volume of 12U. It hosts a tape-like EDT with a cross section of  $2.5\text{ cm} \times 40\text{ }\mu\text{m}$  and total length 430 m. The EDT has a segment of length 410 m made of bare aluminum for electron collections and an inert segment with a length of 20 m. The DD has two modules. The Deployment Mechanism Module (DMM), which has a volume of 5 liters (slightly above 4U), hosts the EDT and it is responsible for the tether's extraction and deployment. The Electron Emitter Module (EEM) has a heaterless hollow cathode (HC) that provides cathodic contact with the ambient plasma. Both modules have their own communication subsystems to send telemetry and receive telecommand. This is an important feature for the preparation of future products because it provides collision avoidance capability to the DD. A telecommand can be sent to the DD to turn on/off the cathode (and activate/deactivate the Lorentz force) in case a collision warning is triggered. The modules are linked by a hold-down and release mechanism (HDRM) that is responsible for the initial separation of the two modules. They both have the same avionics, which is organized into five electronic assemblies: (i) command and data handling assembly, (ii) power assembly, (iii) attitude determination and control assembly, (iv) communication assembly with the telemetry and telecommand radio and antenna, and (v) the payload interface with the avionics dedicated to interface with the DMM and EEM payloads.

The DMM has a novel and compact deployment mechanism (DM) to deploy the thin tape. Two motors allow the controlled extraction of the EDT and following a pre-calculated velocity profile [18]. Besides the avionics and power subsystem, the DMM also has a miniaturized fluid system that provides a separation force and attitude sta-

bilization during the deployment phase. Another key element of the DMM is an in-line damper [10] that is responsible for smoothing tensions peaks during the deployment phase and to dissipate energy passively from the tether oscillations.

The volume of the EEM is a bit larger, about 8U, and it hosts the electron emitter subsystem. The former includes the HC, its operating electronics, and a fluid system for storing the krypton expellant. All of them were specifically developed to meet the rigorous requirements of the DD in terms of volume, power, an electrical parameters (minimum and maximum tether current and HC potential drop). The HC is based on a disc-shaped C12A7 electride insert as the electron emitter and a keeper equipped with a small orifice of 0.5 mm of diameter [5]. The electronics of the electron emitter subsystem has boards for the ignition and the operation of the HC. Regarding the fluid system, it is based on commercial-off-the-shelf elements and has a highly integrated layout based on custom manifolds to reduce the amount of connectors and adapters. It uses krypton and it also features four nozzles as cold gas thrusters, which aid the initial separation process of the two modules of the DD in the tether deployment phase.

The DD is also equipped with elements that will enrich the scientific data to be collected in the in-orbit demonstration but, in principle, they will not be included in future products. An example is the Langmuir probe diagnostic system for the in-situ measurement of the LEO plasma density and temperature. The DD has also a camera to take images of the EDT during the deployment phase.

## 3. TEST PLAN

The objective of the qualification test campaign of the EQM is to ensure that the DD can survive the launch and the harsh conditions of space and function as intended throughout its full mission. Therefore, the DD should be able to detumble itself, prepare the DD for the deployment phase, deploy the EDT, and operate it to accomplish several scientific and technical objectives. This involves a series of rigorous tests to simulate the various environmental stresses the DD will encounter. More specifically, the following test were conducted:

- Functional tests to ensure the correct operation of the DD equipment.
- Proof pressure test to validate that the DD can withstand the operational pressures it will encounter during its mission.
- Leak tests to verify the system pressure boundaries and ensure that there are no leaks that could compromise the DD functionality.

- Vibration and shock tests to ensure the DD can withstand the vibrations and shocks of the launch and the deployment.
- Thermal vacuum cycling tests to evaluate the DD's survivability under thermal conditions in space.
- Electromagnetic compatibility (EMC) tests to validate the electromagnetic compatibility of the different elements of the DD.
- Magnetic dipole test to characterize the position, direction and strength of the residual magnetic dipole.
- HDRM separation test to validate the mechanisms that separate the two modules from their stacked configuration.
- EDT deployment test to validate the proper deployment of the tether.

Figure 1 shows the initial test plan of the EQM, which follows the standard procedure established in the ECSS-E-HB-10-03A Testing guidelines with some peculiarities specific to this project. Test procedures, including the test requirements, were prepared for each test. The test plan starts with the proof pressure and leak tests just after the integration of the fluid system of both modules. After the integration of the avionics of DD, the test plan considers the implementation of functional tests to ensure proper functioning of the hardware and software. They are followed by a partial deployment test of the EDT (about 20 m). Afterwards, with the two modules being stacked, the test plan proposes the vibration, shock, thermal vacuum cycling, EMC and magnetic dipole test. They are followed by the HDRM test to demonstrate the separation of the module and then to repeat the leak test and proof pressure test to ensure the fluid systems survived the stresses endured during the qualification. The plan ends with the full tether deployment test. In parallel, extensive simulation activities on EDT electrodynamic and dynamic and on the attitude determination and control system were carried out. The simulation software developed by the team, like BETsMA v2.0 and FLEX, and the Electrical Ground Support Equipment, were all essential tools to execute them. The dynamics of the in-line damper has been investigated numerically and experimentally [11] and the HC have been also tested intensively in vacuum chamber experiments [19].

Several challenges were overcome to implement the test plan. Besides usual constraints coming from project budget and duration, the participation of four partners was needed in the integration of the EQM and the test campaign: SENER Aeroespacial, Dresden University of Technology (TUD), the University of Padova (UNIPD) and Universidad Carlos III de Madrid (UC3M). Their work was essential due to the specialized knowledge that involved certain elements of the DD (HC, deployment mechanism, fluid system) and access to specific facilities (thermal-vacuum chamber, shaker, tether deployment test facility, etc). This circumstance, that impacted on the schedule of the plan and its complexity, was addressed

by transporting the two modules (or the full EQM) to the different institutions in charge of the tests and also by moving personnel of some institutions to others to implement certain tests. Secondly, although a prototype with TRL 4 was developed in the precursor E.T.PACK project and some elements were intensively tested in the lab, this qualification campaign was the first time that the space-quality DD was tested by the team.

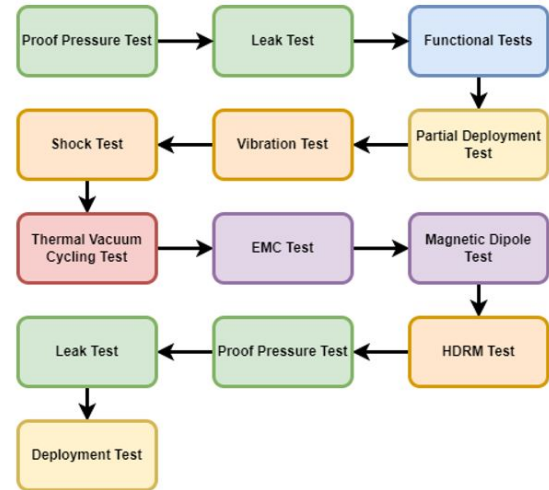


Figure 1. Test Plan of the EQM.

## 4. RESULTS

### 4.1. PROOF PRESSURE TEST

Two proof pressure tests were carried out at TUD. The first test used a hydrostatic pressure calibrator capable of pressurizing a system and measuring the pressure up to 700 bar. The test was conducted for the DMM only to avoid contamination with water of the EEM. This was deemed an acceptable risk, given that the EEM and DMM fluid system share relevant components (e.g. tanks, fill and vent valve, relief valve, pressure regulator) and design approaches. The proof pressure was 1.25 the maximum design pressure, which is 200 bar. Figure 2 shows the DMM during the test. The proof pressure was reached and the relief operation verified.

The second proof pressure test, which was implemented with an argon pressure cylinder with a pressure of more than 250 bars, was carried out for the DMM and the EEM. Its goal was to ensure the system's capacity to maintain the requisite pressure (1.25 the maximum design pressure) and to identify obvious leaks resulting from improper assembly or damaged components. The fluid system was connected to the cylinder with a high-pressure regulator and the ground support equipment fill line. The proof pressure was reached and the vent tool validated for both the DMM and the EEM.

The hydrostatic setup was also used to make design burst



Figure 2. DMM in its containment box during the proof pressure test.

pressure tests of the tanks of the fluid system of the DMM and the EEM. This test was conducted to evaluate the potential risk of a catastrophic burst event during the environmental test campaign. A dedicated tank, which was identical and from the same batch as the tanks used in the EEM and DMM fluid system, was utilized for this test. It was conducted using the hydrostatic pressure calibrator that employs de-ionized water as the working fluid. The fluid system was connected using a dedicated pressure line and the complete setup, excluding the test article, was rated to withstand a pressure of 700 bars. The burst pressure was 300 bar (1.5 the maximum design pressure) and the target pressure was 450 bar (1.5 the burst pressure). The pressure target of 450 bar was reached and no obvious leak was detected, no pressure drop was measured, and no measurable deformation of the tank was observed.

#### 4.2. LEAKAGE TEST

For the leakage measurement, the Pfeiffer ASM 340, a helium leakage detector mass spectrometer, was used in conjunction with a vacuum cylinder. Both the EEM and the DMM were tested but, due to the limitations of the facilities available at the time of testing, a test at maximum design pressure was not feasible. Each module was placed within the vacuum cylinder and the leakage detector drew a vacuum, subsequently measuring the residual helium flow from any leaks (see Fig. 3). The leakage at 8 bar was about  $10^{-3}$  sccm.

#### 4.3. FUNCTIONAL TESTS

The functional tests were divided into two categories: (i) coupling tests prior to the test campaign and (ii) functional tests carried out during other tests of the campaign. This section focuses on the coupling tests. Information



Figure 3. DMM in the vacuum cylinder in the leakage test.

about the functional tests has been integrated in the sections presenting other tests.

The coupling test were organized into 21 categories in order to test the following elements and their interactions among them: electrical power system, drivers of the PCBs, acquisition PCBs, inertial measurement units, gyroscopes, magnetometers, fine sun sensors, coarse sun sensors, GNSS, FRAM and FLASH memories, torquerods, pneumatic valves, thruster valves, motors, radios, inter-OBC communications, antennas, cold gas system acquisition, HC electronics, Langmuir probe system, and camera. For each category, a list of test/verification with an identifier for each test was prepared and also indicating the module (DMM, EEM or both), and the test status. For instance, for the electrical power system, 10 tests were carried out in order to ensure the communication with the OBC, temperature sensors provide meaningful data and react to temperature changes, all output channels can be controlled and have correct voltage levels and delays, etc.

#### 4.4. PARTIAL DEPLOYMENT TEST

The objective of tether deployment tests was to demonstrate that the deployment mechanism could extract the tape smoothly and follow the velocity profile required to align the tape along the local vertical at the end of the deployment phase of the mission. Such a task is performed by two motors [3]. The motor of the orbiter, which is controlled by setting its rotational speed, follows a profile that is based on the required deployment trajectory obtained from simulations [18]. Such a phase lasts for about 1 hour. The motor of the pulleys is regulated through current and determining its optimal current profile involved extensive experimental testing.



Before starting the test campaign of the EQM, extensive testing activities were carried out with the DMM prototype prepared in the precursor E.T.PACK project [13]. As shown in Fig. 4, a custom-designed structure was prepared to suspend and tilt the DMM of both the prototype and the EQM. Such a setup was convenient because it approximate the orbital conditions of weightlessness in the relevant direction while allowing it to naturally release onto the floor with minimal manual handling. The extensive testing with the DMM prototype demonstrated that the results were not sensitive to the specific tilt angle. Several partial deployment tests were conducted to optimize and validate the control laws of the motors during the most critical parts of the deployment profile, i.e., the initial acceleration phase that occurs during the early separation of the two modules, and the transitions between the three coils of the tape spool. In addition, the geometrical features of some mechanical elements internal to the deployment mechanism that align the tape with the extracting pulleys were fine tuned.

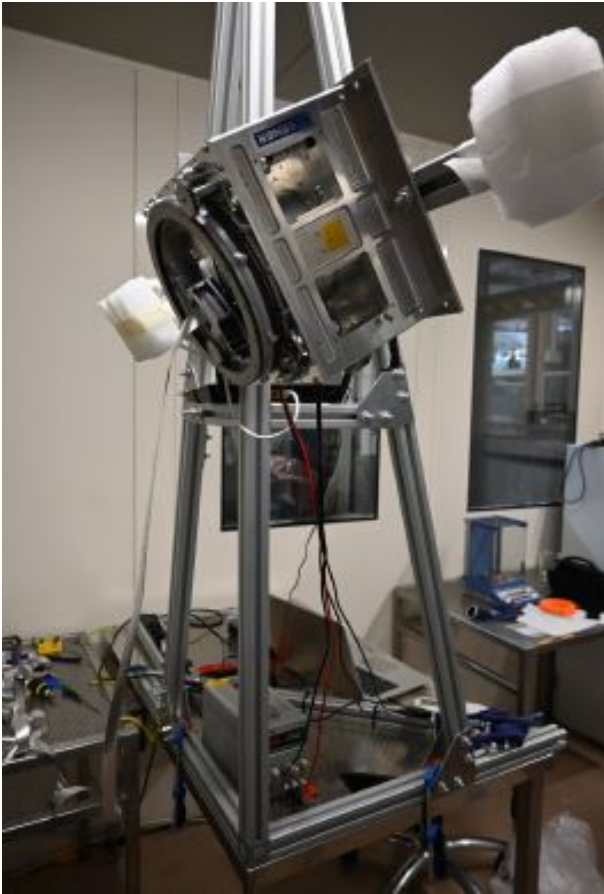


Figure 4. DMM prototype attached to the supporting structure in the CISAS ISO-8 clean room for the partial deployment tests.

#### 4.5. VIBRATION TEST

The vibration test was carried out at SENER facilities with the EQM fully assembled, but only one of the solar panels was tested as they are all of the same characteristics. A jig was designed and manufactured to emulate the cubesat dispenser. The DD was vibrated along the three axes and, for each of them, following the sequence: sine frequency survey (eigen-frequencies detection), sine intermediate level (-6dB respect to qualification), sine qualification level (0dB), sine frequency survey (eigen-frequency detection), quasi static load, sine frequency survey (eigen-frequency detection), random low level (-10dB respect to qualification), random intermediate level (-6dB respect to qualification), random qualification level (0dB), and sine frequency survey (eigen-frequency detection). The levels selected for the mechanical environment to test the EQM of E.T.PACK-F are those of Vega-C (see Table 1). A V875-640 LDS shaker with a SPA32k amplifier was used in the test (see Fig. 5). Two uniaxial accelerometers and seven triaxial accelerometers were installed before the tests at strategic positions like the DDM and EEM structure panels, the DMM orbitator, at the interface of the HDRM, and the DMM and EEM avionics interface planes.

The first main frequencies in the x, y and z axes measured in the tests were 797, 273 and 206 Hz, respectively. Therefore, the DD was compliance with the stiffness criterion (frequency larger than 120 Hz). The EQM withstood the sine, quasistatic, and random qualification levels in all directions without degradation.

Test	Qualification		Acceptance	
	Factors	Duration Rate	Factors	Duration/ Rate
Static (QSL)	1.25	N/A	N/A	N/A
Sine	1.25	2.0 oct/min	1.0	4.0 oct /min
Random	2.25	120s per axis	1.0	60s per axis

Table 1. Vega-C test factors, rate and duration.

Functional tests were carried out in the avionics system to ensure its proper functioning after the vibration tests. They involved all the elements mentioned in the coupling test and other like for instance the kill switch, and the latch vales, among others. All the test were successful, except that the serial communication with the radio reported an error due to a misconnection of serial wire with the radio end during the integration process. Special care will be taken during the integration of the Flight Model (FM) of the DD to avoid the error.

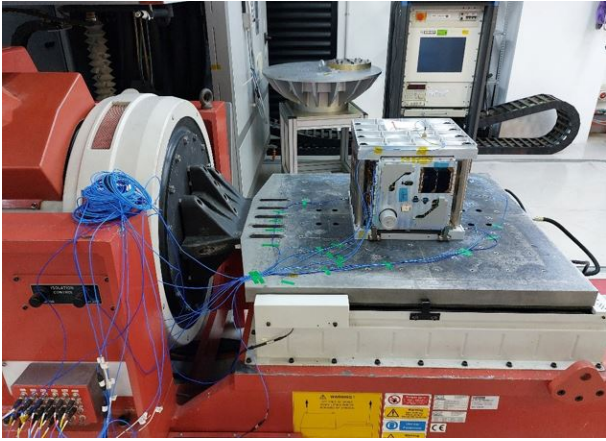


Figure 5. Vibration test of the DD (y-axis configuration) at SENER facilities.

#### 4.6. SHOCK TEST

The EQM, fully assembled but with only one solar panel, was tested at SENER facilities with a jig specially designed and manufactured to emulate the dispenser. A shock test bench, able to reproduce the effects of the pyrotechnical loads on spacecraft equipment, was used. The DD was mounted in a resonant bi-plate that was hit by an impacting object (drop mass). The shock levels, as well as the test factors, were gathered from Vega-C User's Manual. They involve a test factor of 3dB and 2 actuations. The qualification flight limit levels were 56.4, 1100 and 1100 g for frequencies equal to 100, 2000 and 10000 Hz, respectively.

The DD was placed in the shock table as shown in Fig. 6 and two triaxial accelerometers were installed in the baseplate of the DD. Several shocks were performed until the desired levels were acquired in all axis as means of calibration. Since the results are very sensitive to the setup in the shock tests, it was difficult to replicate the exact shock requirements. Nonetheless, the actuation curves of the two accelerometers in all axes laid within the reasonable limits of the shock response requirements. The DD withstood without degradation the shock test. After the shock test, the DD passed successfully through the same set of functional tests explained in Sec. 4.5.

#### 4.7. THERMAL VACUUM CYCLING

The DD, fully assembled but with only one solar panel, was tested at SENER facilities in a thermal vacuum chamber with several thermocouples to measure the temperature during the cycling. They were placed at strategic positions like in the avionic bay of the EEM, next to the batteries and the OBC of the EEM and the DMM and at the canister of the DMM. The operational limits were selected based on previous thermal analysis. The temperature limits obtained in the thermal analysis were modified by  $+10^{\circ}/-10^{\circ}$  (upper limit/lower limit) to acquire the de-



Figure 6. DD in the shock test setup at SENER facilities.

sign temperatures. Those design temperatures were modified an additional  $+10^{\circ}/-10^{\circ}$  (upper limit/lower limit) to set the qualification temperatures shown in Table 2.

Following ECSS testing specification, the EQM was subjected to 4 thermal cycles. The thermal sequence is as follows

1. At room temperature and pressure, the DD was mounted into the chamber, the avionics were turned on and a health check was performed to verify functionality. The avionics were then turned off.
2. The DD was brought up to the maximum non-operational temperature.
3. The DD was brought down to the maximum operational temperature. The avionics were turned on and a functional check was performed. The avionics were turned back off.
4. The DD was brought down the minimum non-operational temperature.
5. The DD was brought up to the minimum operational temperature. The avionics were turned on and a functional test was conducted.
6. Three more cycles were performed between maximum and minimum operational temperatures.
7. In the last cycle, functional tests were performed both at the maximum and minimum operational temperatures.
8. The DD was brought back to room temperature and pressure. A health check was performed to verify functionality.
9. The avionics were turned off and the DD was taken out of the chamber.

The pressure during the test was less than  $10^{-5}$  hPa. The DD withstood without degradation the vacuum pressure and the thermal cycling and all the requirements were met considering both the design and execution of the test. All the functional tests after the test were successful except the tests of the serial communication of the electrical power systems of both modules and a magnetometer of the DMM. In the case of the DMM, a malfunctioning occurred during the integration of the system into the chamber. In the case of the EEM, the serial port connector was deliberately removed from the EPS due to configuration issues. Regarding the magnetometer, we detected that faulty measurements were taken during the tests and the magnetic field data was not always updating correctly. By a close examination it was detected that the PCB of the magnetometer suffered damaged in one of the magnetic sensing integrated circuits and the origin of the damage was attributed to the integration process. Preventive measures in the integration process of the FM will be taken to avoid these issues with the magnetometer and the serial communication of the electrical power systems.

Temperature	Value
$T_{NO-MAX}$	+45 °C
$T_{NO-MIN}$	-30 °C
$T_{O-MAX}$	+37 °C
$T_{O-MIN}$	-23 °C

Table 2. EQM Qualification Temperatures.

## 4.8. ELECTROMAGNETIC COMPATIBILITY (EMC)

### 4.8.1. CONDUCTION TEST

The EQM was subjected to the following EMC conductive/discharge testing: (i) bonding and grounding to measure the resistance between any point on the equipment housing and ensure that the resistance is lower than 5 mΩ and (ii) susceptibility to electrostatic discharges (ESD) into the chassis. The latter was studied by applying an electrostatic discharge to the satellite structure to assess its survivability. The DD should not be susceptible when subjected to the contact discharge current waveform at 8kV explained in the ECSS-E-10-03C (Rev 1).

The bonding and grounding test was conducted with a Miliohmmeter CROPICO DO4002. More than 150 points were selected for measurement, including reference points, metallic parts and structural elements (screws). For all of them the resistance was lower than 5 mΩ proving that the DD was properly grounded. Regarding the ESD test, it was carried out with the ESD Simulator (Discharge Gun) of Rohde& Schwarz. The discharge was set to 9kV to meet the discharge current curve of ECSS-E-ST-20-07. Although 8kV was the requirement,

9 kV were applied to meet the 30 A peak of discharge current. A total of 30 discharges were applied in the positive and negative direction (60 discharges in total). The DD was on during the discharges and it did not exhibit any malfunction during the execution of the discharges, thus proving its immunity.

Functional tests were carried out after the ESD test. They were all successful except for a capacitor of the HDRM, which was damaged due to the ESD discharge. An ESD protected circuit will be implemented on the FM board to avoid damage to the HDRM capacitor (find more information in Sec. 4.9).

### 4.8.2. RADIATION TESTS

The EQM fully assembled, in stacked configuration, and without solar panels was subjected to the following EMC radiative testing: (i) radiated emission test, electric field 30MHz to 18GHz, (ii) radiated susceptibility test, magnetic field 30Hz to 100KHz, (iii) radiated susceptibility test, electric field 30MHz to 18GHz, and (iv) autocompatibility test. The latter is aimed at testing the transmission and reception of both UHF and S-band antennas and reception systems. Figure 7 shows the DD during the radiated emission test.



Figure 7. DD in the radiated emissions test.

The measurements for radiated emissions, taken at all frequencies both for vertical and horizontal polarization, were all well below the limits established in ECSS-E-ST-20-07C Rev.2. The DD did not exhibit failure, malfunction, unintended responses nor degradation of performances during and after its subjection to radiated magnetic fields in all faces neither when subjected to radiated electric fields in all tested frequencies for both horizontal and vertical polarization. Regarding autocompatibility, the transmissions of the UHF and S-band antennas occurred at the expected frequency. In relation to reception, during and after the test, the DD operated without loss or degradation of performance when subjected to signals with frequencies 400 MHz (UHF) and 2.3 GHz (S-band)



with horizontal and vertical polarization. All the functional tests carried out after the radiative EMC tests were successful.

#### 4.8.3. MAGNETIC DIPOLE CHARACTERIZATION

The magnetic dipole characterization, which is very important for the detumbling and tether deployment stabilization phases [8], was carried out in IMA Velayo Facilities. A system of Helmholtz coils (Helmholtz Cage) was used in all three spatial directions to create an area that compensates for the Earth's magnetic field. For the tests, the DD was preconfigured with eight different operational modes (from mode 0 to mode 7), where different components of the DD were activated in each mode to calculate the change in dipole for each operational configuration. The magnetic field was measured using two types of sensors. The first is a fluxgate magnetometer with an experimental resolution of 100 nT, used to determine the magnetic field strength. The second sensor is an axial Hall probe, strategically positioned just above the fluxgate sensor. This Hall probe serves to compare the values obtained from the fluxgate magnetometer and to verify that the compensation of the Earth's magnetic field is consistently maintained throughout the measurement process. Both sensors were calibrated prior to starting the measurements. By using the measured values, the total magnetic moment was calculated for each mode. It was found that the modes of operation primarily affect the dipole moment of the DD along the Z-axis. No significant changes in the magnetic field were detected along the X and Y axes across any operational mode.

After the magnetic dipole was measured, the magnetic neutralization process (deperm) was carried out. This process applies an AC magnetic field to the DD to remove any residual magnetism from its elements after exposure to other magnetic fields. The magnetic field was then measured with the DD turned off and the magnetic moment was calculated. The value of the magnetic moment before and after deperm were  $0.0122 \text{ Am}^2$  and  $0.0269 \text{ Am}^2$ , respectively. It was concluded that some components of the DD can be magnetized by the fields emitted by other components but this magnetization is minimal. Afterwards, the magnetic field of the DD was measured after activating the magnetorquers, which are the components that generate the strongest magnetic fields within the DD and are most likely to magnetize other elements. A magnetic moment of  $0.0191 \text{ Am}^2$  was found, corroborating that some components may become magnetized during the operation of the magnetorquers, but this magnetization does not result in a significant magnetic field.

Independently of this test, UC3M characterized the magnetic dipole of the DD by using a different experimental setup that does not need to compensate for the Earth magnetic field (see Figure 8). The center of the dipole, its direction and the intensity were measured for the 8 modes and the results were consistent with the ones obtained with the Helmholtz Cage setup (see details in Ref.

[17]). Functional tests were not required after magnetic dipole characterization because these tests do not affect the DD in any way as they just consist of taking measurements.

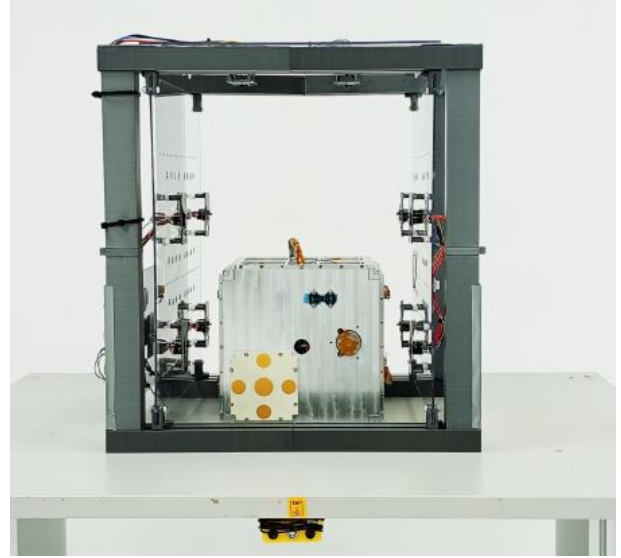


Figure 8. DD in the dipole characterization setup at UC3M.

#### 4.9. HDRM Test

The hold-down and release mechanism (HDRM) was tested by using the EQM fully assembled (no solar panels) and in stack configuration. As shown in Figure 9, a specific setup was built to hold the DD during the test. A counterweight was placed in a pulley system to mimic the zero-gravity condition that the spacecraft will feel in space. In this setup, the DMM is fixed and the EEM is 'freely' released once the HDRM is activated. However, when the command was sent, the HDRM did not activate because the HDRM capacitor was damaged during ESD test (see Sec. 4.8).

After the error was detected, the two modules were separate for inspection. Besides the damage in the capacitor, three issues were identified: (i) a small displacement of the tape in the canister, (ii) the attachment of the modules, involving the in-line damper and shock absorber via Kevlar strings, was not strong enough, and (iii) the gear of the deployment mechanism did not rotate properly. After analysis, it was found that the gears were constraint from proper rotation due to the bearings being dirty.

Due to these issues, it was decided to make changes to correct all of them and adapt the test plan shown in Figure 1 to include a delta-qualification. It involves repeating the vibration test, and continue the test plan with the HDRM separation test and the full tether deployment test. Since the errors found after the HDRM test were not relevant for the subsequent proof-pressure and leakage test, they were carried out normally before starting



the delta-qualification. These tests, that were both successful, were similar to the one explained in Secs. 4.1 and 4.2.

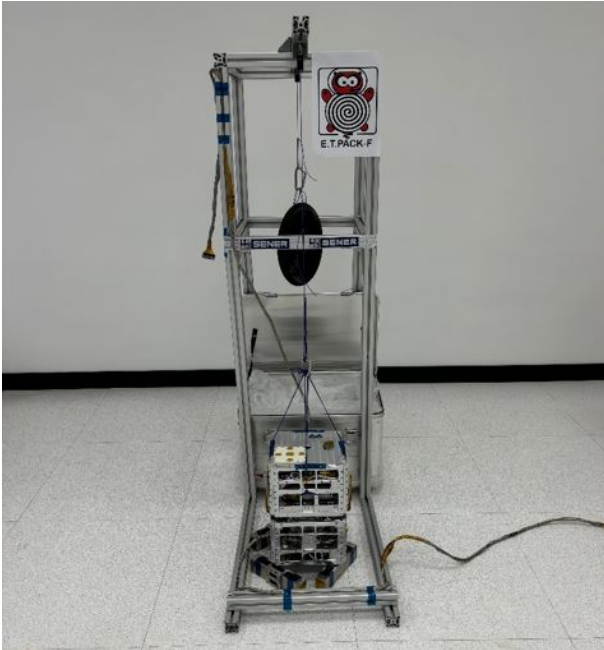


Figure 9. DD in HDRM test at SENER.

#### 4.10. DELTA-QUALIFICATION VIBRATION TEST

The issues detected after the HDRM test triggered the following changes in the EQM. Firstly, to avoid tether displacements in the vibration test, the spooling machine used by UNIPD to prepare the tether coils was modified to increase the tether tension at the coils. Secondly, a new attachment system for the junction of the in-line damper – shock absorber – modules was installed. Such a solution was tested to a force up to 50 N. Thirdly, the bearings were cleaned and space lubricant was applied. A new design solution was developed to avoid contamination in the bearings of the FM. In addition, the HDRM system was recharged, the capacitor fixed, and the modules were stacked again.

The vibration test explained in Sec. 4.5 was repeated completely for the EQM and it was compliant with all the requirements of the test. Functional tests were carried out and all of them were successful, except an issue again in the capacitor of the HDRM. It did not survive the vibration test because it was improperly mounted. For the FM, the proper installation procedure will be followed to avoid damage. The capacitor was replaced to be able to carry out the delta-qualification HDRM separation test.

#### 4.11. DELTA-QUALIFICATION HDRM SEPARATION TEST

The HDRM test was successful. The two modules (DMM and EEM) detached from each other upon command proving the proper functioning of both the HDRM mechanism and the deployment routine software. About 18 cm of tether came out after the modules detachment, as desired, demonstrating the correct functioning of the pull-out mechanism.

#### 4.12. FULL TETHER DEPLOYMENT TEST

Before conducting the full deployment tests, some preliminary tests revealed the need to implement modifications to the current profile of the pulleys motor and of the spool canister. Indeed, the first vibration test evidenced the need to increase the tape pull force during its winding onto the spool to avoid coil slippage during the test. The increased pull force, in turn, required a redesign of the canister to avoid buckling effects. A second effect observed after vibration test was an increase in the friction torque on the orbitator bearings. This led to a different optimization of the unwinding system to maintain the centering of the tape on the pulleys throughout the whole deployment.

A series of partial deployment tests were conducted to validate the new system configuration and ensure the overall reliability of the deployment process. For the full deployment tests, the DMM EQM was mounted on the same structure used for the partial deployment tests of the DMM prototype. The tests were conducted in a clean room (ISO-8) at ambient temperature and pressure. Finally, two complete end-to-end tests of the full tether deployment were successfully performed, with a smooth tape extraction that remained well-aligned as it exited the pulleys.

Following the full deployment tests, at the time of writing this paper, UNIPD is carrying out additional partial deployment tests with the DMM EQM inside a vertical Thermal Vacuum chamber (see Figure 10), with the main objective of proving the reliability of the deployment mechanism under conditions representative of those expected in orbit. Specifically, three partial deployment tests will be conducted: 1) one test in vacuum (absolute pressure about  $10^{-5}$  Pa) at ambient temperature (about  $16^{\circ}\text{C}$ ); 2) one test in vacuum at a temperature of  $+39^{\circ}\text{C}$  (hot case); and 3) one test in vacuum at a temperature of  $-23^{\circ}\text{C}$  (cold case).

### 5. CONCLUSIONS

The extensive qualification campaign of the EQM has been a key activity to validate the fulfillment of the requirements of the DD and learn about the behavior of

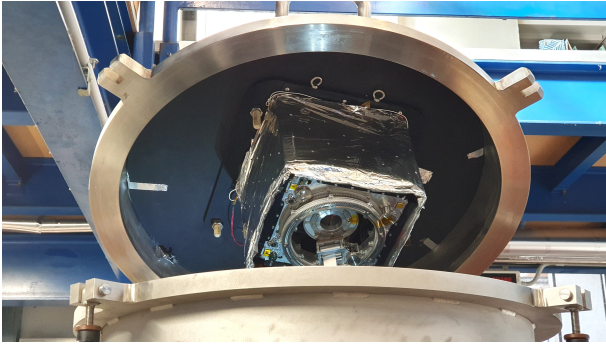


Figure 10. DMM EQM attached to the upper cover of the CISAS vertical thermal vacuum chamber for thermal vacuum partial deployment tests.

all its elements in variety of mechanical, thermal, vacuum and radiative environments. The campaign included proof pressure and leak tests, tether partial deployment test, two vibration tests, shock tests, thermal vacuum cycling, electromagnetic compatibility (conductive, radiative and magnetic dipole characterization) tests, separation test of the modules, and full tether deployment test. After each of them functional tests were also carried out. These tests were complemented with extensive simulation analysis and tests on individual subsystems like for instance the hollow cathode, the communication subsystem, and the in-line damper among others. The tests provided a set of invaluable data that will impact positively on the Flight Model (FM). Important lessons were learned related to the capacitor of the HDRM (integration procedure and adding an electrostatic discharge protection circuit). The need for increasing the tether tension in the canister, which was validated by the delta-qualification vibration test, as well as the reinforcement of the canister structure to withstand such a tension without buckling and adding a labyrinth to avoid the contamination of the bearings, were also pivotal conclusions that were extracted from the qualification campaign. Finally, the extensive tests of the tether deployment allowed to improve the elements of the deployment mechanism and fine tune the control laws for the motors. The two successful end-to-end full tether deployment tests achieved after these modifications provide confidence about the robustness of the deployment mechanism and its control laws.

The FM, which is currently in its manufacturing phase, benefits from all these lessons learned. After integration, it will pass through the acceptance test campaign. Besides the test levels, it involves the same set of tests explained in this work, except for the shock test, electrostatic discharge and radiative tests, the dipole characterization. Such a campaign will finish with the full tether deployment test. Afterwards, the tape spool will be prepared, installed on the FM and the latter one re-stacked to be ready for the flight. The in-orbit demonstration is planned in Q2 2026. It will be launched by AVIO thanks to a flight opportunity funded by the ESA/EC Flight Ticket Initiative.

## ACKNOWLEDGMENTS

This work was supported by the European Union's Horizon Europe Research and Innovation Programme (No 101058166, E.T.PACK-F project). The authors thank the following team members of the E.T.PACK-F project that participated in the qualification campaign of the deorbit device: J.P. Wulfkühler, E. Berka, J. Hertel, R. Neger, S. Eisenhut, D. Cruces, A. Velasco, E. Lorenzini, B. Saggin, A. Brunello, G. Polato, S. Chiodini, M. Ghedin, G. Anese, S. Salmistraro, G. Sharifi, J. Gonzalez-García and B. Vatankhahghadim.

## REFERENCES

- Berthet, M., et al. (2024) Space sails for achieving major space exploration goals: Historical review and future outlook. *Progress in Aerospace Sciences*, **150**, 101047.
- Brunello, A., Anese, G., Chiodini, S., Colombatti, G., Polato, G., Salmistraro, S., Valmorbida, A., and Lorenzini, E. (2024) The deployment mechanism of the e.t.pack deorbit system: Functional and qualification tests. *Acta Astronautica*, **226**.
- Brunello, A., Anese, G., Chiodini, S., Colombatti, G., Polato, G., Salmistraro, S., Valmorbida, A., and Lorenzini, E. (2025) The deployment mechanism of the e.t.pack deorbit system: Functional and qualification tests. *Acta Astronautica*, **226**, 39–47.
- Castronuovo, M. M. (2011) Active space debris removal—a preliminary mission analysis and design. *Acta Astronautica*, **69**, 848–859.
- Drobny, C., Wulfkühler, J.-P., and Tajmar, M. (2022) Characterization of a low current heaterless c12a7 electrified hollow cathode for an electrodynamic tether deorbiting device. *37th International Electric Propulsion Conference*, 06, Massachusetts Institute of Technology, Cambridge, USA.
- Commission, F. C. (2022), Space innovation ib docket no. 22-271 mitigation of orbital debris in the new space age ib docket no. 18-313.
- Fanfani, A. (2017) D-sat mission: an in orbit demonstration of satellite controlled re entry.
- Garcia-Gonzalez, S. and Sanchez-Arriaga, G. (2022) Attitude determination and control for the deployment preparation phase of a space tether mission. *Acta Astronautica*, **193**, 381–394.
- Grossi, M. D. (1995) Plasma Motor Generator (PMG) electrodynamic tether experiment. *Final Report of NASA Grant NAG9-643*, pp. 1–4.
- Lorenzini, E., Olivieri, L., Andrea, A. V., and Alice Brunello, G. S. (2022), Damper device and connecting apparatus. PCT/1B2022/060199.
- Polato, G., Urbinati, M., Valmorbida, A., Anese, G., Brunello, A., Salmistraro, S., Chiodini, S., Colombatti, G., and Lorenzini, E. (2025) Experimental test and numerical validation for evaluating the dynamics of the

in-line damper for the e.t.pack-f project. *Acta Astronautica*, **228**.

12. Sánchez-Arriaga, G., Sanmartín, J., and Lorenzini, E. (2017) Comparison of technologies for deorbiting spacecraft from low-earth-orbit at end of mission. *Acta Astronautica*, **138**, 536–542, the Fifth International Conference on Tethers in Space.
13. Sánchez-Arriaga, G., Naghdi, S., Wätzig, K., Schilm, J., Lorenzini, E., Tajmar, M., Urgoiti, E., Castellani, L. T., Plaza, J., and Post, A. (2020) The e.t.pack project: Towards a fully passive and consumable-less deorbit kit based on low-work-function tether technology. *Acta Astronautica*, **177**, 821–827.
14. Sánchez-Arriaga, G., Lorenzini, E. C., and Bilén, S. G. (2024) A review of electrodynamic tether missions: Historical trend, dimensionless parameters, and opportunities opening space markets. *Acta Astronautica*, **225**, 158–168.
15. Sanchez-Arriaga, G., et al. (2024) The E.T.PACK-F project: towards a flight-ready deorbit device based on electrodynamic tether technology. *AIAA SCITECH 2024 Forum*.
16. Sanmartin, J., Martinez-Sanchez, M., and Ahedo, E. (1993) Bare wire anodes for electrodynamic tethers. *Journal of Propulsion and Power*, **9**, 353–360.
17. Sharifi, G., Gonzalez-García, J., and Sánchez-Arriaga, G. A low-cost experimental setup for the determination of the residual magnetic dipole of small satellites. (*submitted*).
18. Valmorbida, A., Olivieri, L., Brunello, A., Sarego, G., Sánchez-Arriaga, G., and Lorenzini, E. (2022) Validation of enabling technologies for deorbiting devices based on electrodynamic tethers. *Acta Astronautica*, **198**, 707–719.
19. Wulfkühler, J.-P., Berka, E., Hertel, J., Nerger, R., Tajmar, M., Cruces, D., Machon, A., and Velasco, A. (2024) A heaterless c12a7 electrified-based hollow cathode electron emitter system for microsats. *38th International Electric Propulsion Conference (IEPC)*, 06.